

# Atomic Force Microscope

Sing Teng Chua  
Mayar Mohamed  
Department Physics and Astronomy  
Waterloo University

## CONTENTS

<b>I</b>	<b>Introduction</b>	1
<b>II</b>	<b>THEORETICAL BACKGROUND</b>	2
<b>III</b>	<b>EXPERIMENTAL DESIGN AND PROCEDURE</b>	2
III-A	Description of the apparatus . . . . .	2
III-B	Description of the experimental procedure . . . . .	2
<b>IV</b>	<b>ANALYSIS</b>	3
IV-A	Method of analysis . . . . .	3
IV-A1	Calibration grid sample . . . . .	3
IV-A2	CD sample . . . . .	5
IV-A3	SCA chip sample . . . . .	6
IV-B	Discussion of results . . . . .	7
<b>V</b>	<b>Conclusion</b>	7
<b>References</b>		7

## LIST OF FIGURES

1	The AFM feedback loop consisting of a laser detection system and a compensation network which monitors the sample or cantilever height. [1] . . . . .	1
2	The experimental set-up of AFM under (a) static and (b) dynamic mode . . . . .	2
3	User interface of Easyscan 2 with three primary tabs, namely the “File” tab, the “Acquire” tab and the “Analysis” tab . . . . .	3
4	Nanosurf 5 $\mu\text{m}$ square pattern with a 10 $\mu\text{m}$ period grid . . . . .	3
5	The scanned grid sample . . . . .	3
6	Measuring the periodicity of the vertical direction . . . . .	4
7	Cross section of the grid sample - Periodicity . . . . .	4
8	Zooming on the grid sample . . . . .	4
9	3D image of the zoomed grid sample . . . . .	4
10	The cross-section of the zoomed grid sample . . . . .	5
11	CD sample . . . . .	5
12	3D view of the CD sample . . . . .	5
13	Measuring Periodicity of the CD sample . . . . .	5
14	Cross section of the CD sample . . . . .	6
15	SCA Sample . . . . .	6
16	Cross section of the SCA Sample . . . . .	6
17	Dimensions of the SCA Sample . . . . .	6
18	(a) unfiltered scan vs (b) glitch and noise filter applied on SCA scan image . . . . .	6

## LIST OF TABLES

I	Classifications of various forces which govern the working principles of AFM . . . . .	2
II	Material properties and physical dimensions of different cantilevers . . . . .	2
III	AFM mode and scanning parameter for different specimens studied . . . . .	3
IV	Manufacture grid sample parameters . . . . .	3
V	periodicity scanning parameter . . . . .	4
VI	Zoomed sample scanning parameters . . . . .	5
VII	periodicity scanning parameter for the CD sample . . . . .	5
VIII	SCA dimensions measurements . . . . .	6
IX	Area roughness measurements for SCA sample . . . . .	7

# Atomic Force Microscope

**Abstract**—Atomic force microscope (AFM) was used to study a calibration grid, a CD stamper and a SCA chip under static and dynamic mode respectively.

Atomic force microscope (AFM) was used to study a calibration grid, a CD stamper and a SCA chip under static and dynamic mode respectively.

## I. INTRODUCTION

Atomic Force Microscope is categorized under scanning probe microscope (SPM) which investigates and produces the image of a sample surface down to the molecular scale. AFM can produce an imaging resolution within fractions of nanometers, emerging as a popular microscopy method known for its simple operation, versatile set-up, high speed, relatively low cost without a need for vacuum system and the ability to study an electrically insulating surface.

Cantilever is the primary component used to detect microscopic deflection caused by different interactions between the sample surface and the force sensor in AFM. A sharp pyramidal or conical tip mounted at the end of the cantilever is sensitive in detecting the force with the sample surface, enabling accurate topographic scanning. A standard tip made up of silicon or silicon nitride can be either in continuous or intermittent contact with the sample during raster scanning under Contact or Dynamic (Tapping) mode respectively. To attain sufficiently high lateral resolution, a tip has to be extremely sharp between 1 and 10 nm in diameter. Functional coating of AFM tip for magnetic, electrical or bio-active application is also possible.

The amount of deflection of a cantilever is quantified with the use of a laser beam that is reflected from the back of the cantilever and displaced on a position-sensitive photodetector (PSPD). Since the cantilever-detector distance is generally thousands of times the length of the cantilever, the PSPD can measure the tip displacement below 1 nm with significant magnification of the tip motion by the optical lever. Given the extremely small displacement, the system is assumed to be within the elastic limit, thus validating the use of Hooke's Law  $F = k z$  where  $F$  is the force applied to the tip,  $k$  is the spring constant of the cantilever and  $z$  is the vertical displacement of the tip.

In addition, a piezoelectric scanner helps to maintain the vertical position of the sample relative to the tip during horizontal scanning of the sample. This is attributed to the ability of piezoelectric material to expand or contract in response to the applied electrical voltage from the feedback loop. This function is imperative in producing a topographic image whereby the cantilever deflection is used as input to the feedback circuit to maintain constant vertical displacement between the tip and the sample across the entire surface.

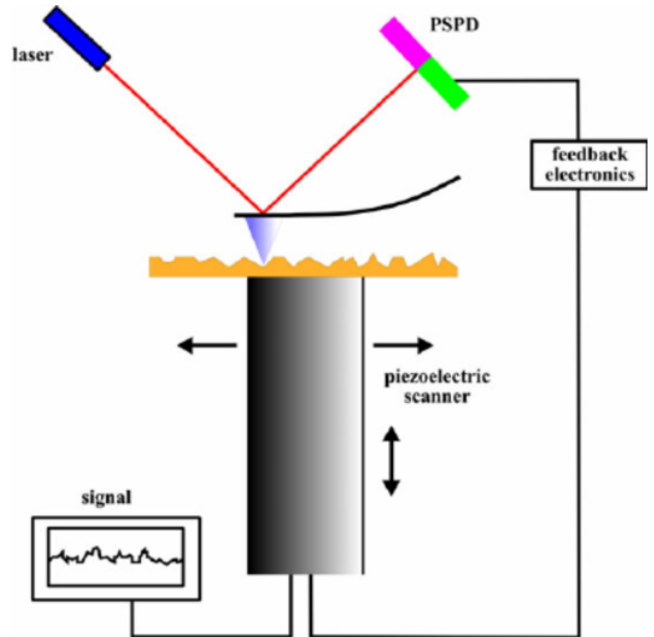


Fig. 1. The AFM feedback loop consisting of a laser detection system and a compensation network which monitors the sample or cantilever height. [1]

AFM can be operated under a number of analytic modes, namely contact (or static), non-contact and intermittent-contact (or dynamic) mode. In the contact mode, the tip is extremely close to the surface to make use of the repulsive steric force. While the contact mode is most useful for hard surfaces, the probe tip is susceptible to contamination from removable material on the surface in contact. In addition, excessive force in contact mode can potentially blunt the tip and damage the sample surface. On the other hand, long-range forces are utilised in the non-contact mode with considerably larger separation between the tip and the surface (1 nm). The cantilever resonance frequency can be changed by the interaction force gradient to be detected and analysed accordingly. While the non-contact mode minimises tip or surface damage, the attractive Van der Waals forces are substantially weaker than the short-range forces used in contact mode. As a result, the non-contact method is more sensitive to environmental variations and surrounding moisture vibrations. For instance, the effect of capillary force exerted on the probe during its withdrawal from the surface becomes very significant, to the point of data interference. A balanced trade-off between contact and non-contact modes is the dynamic or intermittent-contact mode. In this case, the tip is brought into contact with the surface momentarily for high resolution and then lifted off to prevent dragging across the surface. These two steps are

repeated in alternating sequence, normally at a frequency of 75 to 300 kHz. Using a piezoelectric crystal, the cantilever is oscillated near its resonance frequency in ambient air, but the oscillation amplitude decreases upon contact with the surface owing to energy loss. This amplitude reduction can be analysed to study the surface properties and morphology. Thus, dynamic mode can achieve reasonable high resolution while eliminating tip-related issues caused by static mode.

## II. THEORETICAL BACKGROUND

There are several forces between the sample surface and the tip, largely separated into two categories, namely long and short range. These forces are summarised in Table 1 below.

TABLE I. CLASSIFICATIONS OF VARIOUS FORCES WHICH GOVERN THE WORKING PRINCIPLES OF AFM

Long Range	Van der Waals, electrostatic, capillary
Short Range	Interatomic repulsion, chemisorption, metallic adhesion, friction

One basic working principle of AFM requires that the cantilever's spring constant is weaker than that of interatomic bonds [2], to ensure that the surface atoms will not be displaced in the vicinity of the approaching cantilever tip. The origin of these intermolecular interactions is primarily electrodynamic. For instance, the van der Waals' attraction can be described by the interatomic pair potential  $w = \frac{C}{r^6}$ , where C is a constant while r is the intermolecular distance. The strong attractive capillary force ( $10^{-8}$ ) at the tip-sample interface arises from the curvature-induced condensation of atmospheric vapor or the adsorbed moisture layer, whose thickness varies with the relative humidity of the atmosphere and the physico-chemical nature of the specimen. The capillary forces can be minimised by operating AFM in a dehydrated inert atmosphere or by immersing the tip entirely in a liquid fluid cell.

The interatomic short-range repulsive forces are proportional to  $r^{-n}$  with n greater than 8. These repulsion forces originated from the Pauli's exclusion principles whereby two electrons with the same spin cannot occupy the same orbital, as well as the incomplete screening of the nuclear charges by two overlapping electron clouds which generates coulombic repulsions. In addition, overlapping wave functions of multiple atoms result in attractive forces of covalent bonds or chemisorption with concentrated electron density between two or more nuclei. Highly delocalised electron clouds tend to overlap when two metallic surfaces come in immensely close vicinity, giving rise to metallic adhesion that decays exponentially with distance. Furthermore, unlike other forces which are normal to the sample surface, friction consists of a component parallel to the surface, providing critical chemical information through the degree of cantilever twisting which depends on the surface composition.

## III. EXPERIMENTAL DESIGN AND PROCEDURE

### A. Description of the apparatus

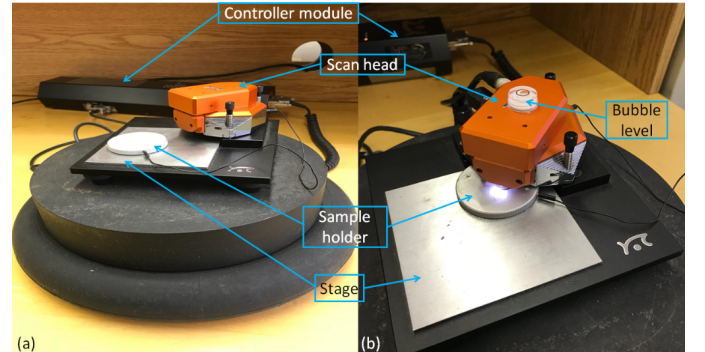


Fig. 2. The experimental set-up of AFM under (a) static and (b) dynamic mode

Different sets of apparatus were used for static and dynamic mode, as shown in Figure 3 2a and 2b respectively. Generally, both AFM consist of a scan head consisting of a cantilever, a disk-shaped sample holder on a square stage and a controller module which is connected to the desktop. The sample holder is a small flat silver disk with a diameter of 5 cm. The sample holder is firmly secured to the stage using a magnet in the base. Two separate cantilever tips are used, namely the SICON-A tip in the static mode and the ACL-A tip in dynamic mode. Both tips are made of n-type silicon by micromachining. The SICON-A tip is longer and thinner but the ACL-A tip has much higher vibration frequency and spring constant. The specifications of two different cantilevers are listed in Table II.

TABLE II. MATERIAL PROPERTIES AND PHYSICAL DIMENSIONS OF DIFFERENT CANTILEVERS

	Length(mu)	Width(mu)	Thickness(mu)	Frequency(kHz)	Spring constant (N/m)
SICON-A	450	49	2.5	11-19	0.1-0.6
ACL-A	225	40	7.8	160-225	36-90

### B. Description of the experimental procedure

The experiment commences with the removal of the calibration grid sample from its container to be placed on the sample holder. The sample holder is secured by magnetic force on the stage beneath scan head. A connection is made between the holder and the right rear corner of the scan head by a thin grounding wire. The microscope controller can be switched on at this point, before initiating the Easyscan 2 software in the desktop. The user interface of Easyscan 2 is illustrated in Figure 3. The primary step is to determine the preparation parameters, namely the scanning mode, the surrounding medium and the type of cantilever used on the "Acquisition" toolbar. The video camera enables synchronised observation of the cantilever tip movement and its distance away from the sample through both top-view and side-view window. After ensuring sufficient clearance between the specimen surface and the cantilever tip by naked eye observation, one can slowly slide the sample holder towards the scan head. A round bubble level is then

placed on the scan head. Three leveling screws are used to adjust the orientation of the scan head until the bubble lies stably in the circle at the center. After that, use the top-view monitoring to search for a relatively blemishless spot on the sample while shifting the sample position along the stage plane very slowly. Once a satisfactory sample area is selected, the video monitoring is set to side-view mode, and the “Advance” function is initiated until the tip comes into close vicinity with the sample surface, as visible from the better focusing of the sample surface at the video background. Meanwhile, the shadow of the tip can be seen on the sample surface. Once the tip and its surface appear immensely close to one another, the automatic “Approach” function can be activated by clicking the button whereby the tip will be brought into optimal contact with the surface. After setting the parameter such as scanning size and speed, one can press the “Start” button for probe scanning to begin and the “Finish” button for automatic termination after one full scanning is completed.

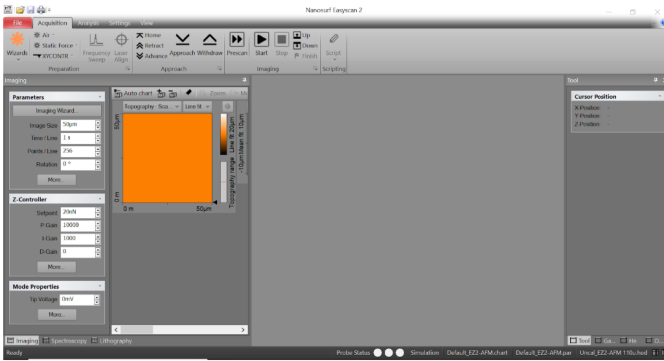


Fig. 3. User interface of Easyscan 2 with three primary tabs, namely the “File” tab, the “Acquire” tab and the “Analysis” tab

After image analysis is completed, sample replacement is performed using the “Withdraw” and “Retract” button to raise the probe tip to an adequate height above the sample. The second sample studied under the static mode is a CD stamper, which is loaded onto the AFM using similar preparation method as aforementioned. Similarly, the Switched Capacitor Array (SCA) chip is studied with the same set of procedures under the dynamic mode. However, it must be noted that during the dynamic mode the scan head was not kept at perfect ground level. The rear end of the scan head was raised to a higher level than the front end which is nearer to the tip because the base of the scan head tends to contact the sample surface before the tip is sufficiently close to the surface, thus impeding proper operation of AFM. On the other hand, if the scan head was tilted at an angle with the probe tip touching the sample first, the problem is solved. Nonetheless, artifacts such as astigmatism could occur as a result, as further illustrated in later section. The scanning parameter for three different samples are summarised in Table III.

TABLE III. AFM MODE AND SCANNING PARAMETER FOR DIFFERENT SPECIMENS STUDIED

	Calibration grid	CD stamper	SCA chip
Mode	Static	Static	Dynamic
Scanning size	50μm x 50 μm	25 μm x 25 μm	60 μm x 60 μm
Scanning speed	1 sec per line	1 sec per line	1 sec per line

## IV. ANALYSIS

### A. Method of analysis

The primary method used to analyze the data was to find the mean and standard deviation of the parameters the patterns and compare it to the manufacture parameters.

1) *Calibration grid sample*: We obtained Calibration grid sample data from Nanosurf manufacturer:

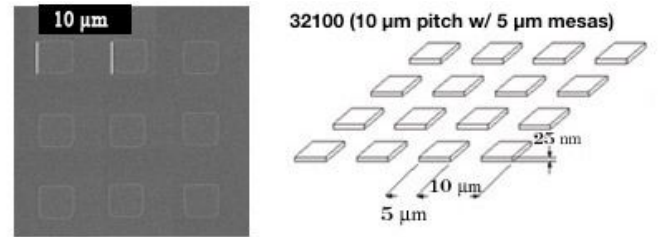


Fig. 4. Nanosurf 5 μm square pattern with a 10 μm period grid

TABLE IV. MANUFACTURE GRID SAMPLE PARAMETERS

periodicity (μm)	Step height(nm)	Square length(μm)
10	25	5

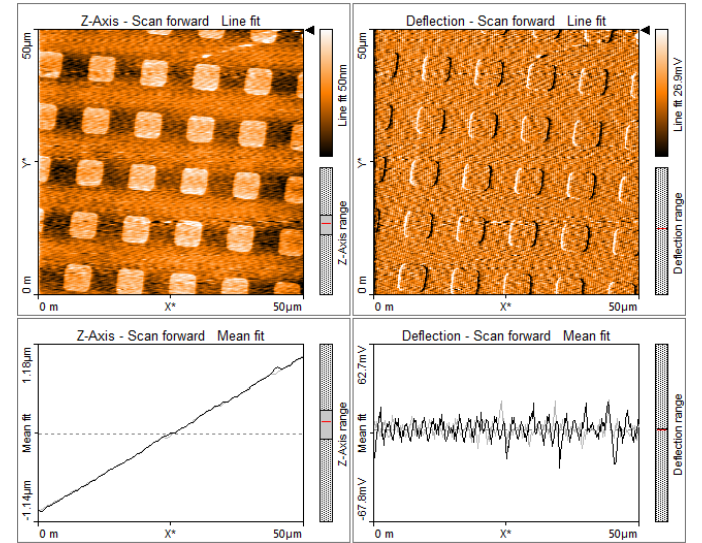


Fig. 5. The scanned grid sample

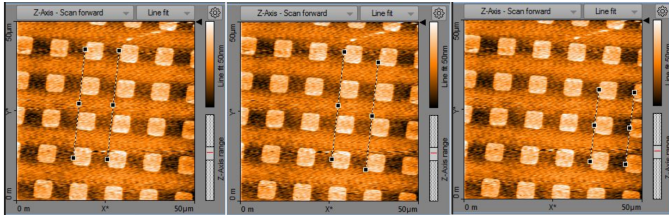


Fig. 6. Measuring the periodicity of the vertical direction

TABLE V. PERIODICITY SCANNING PARAMETER

	Vertical periodicity(mu)	Horizontal periodicity(mu)
1st	9.653	9.639
2nd	9.846	9.799
3rd	10.09	9.418
Average	9.863	9.619
Standard Deviation	0.219	0.1913

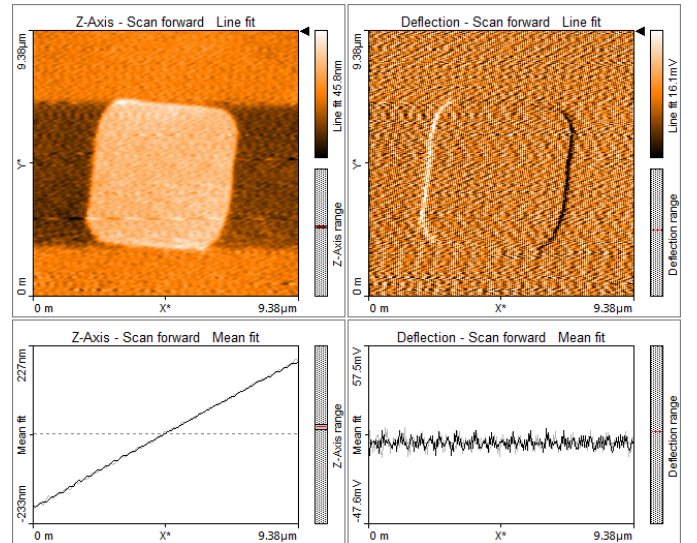


Fig. 8. Zooming on the grid sample

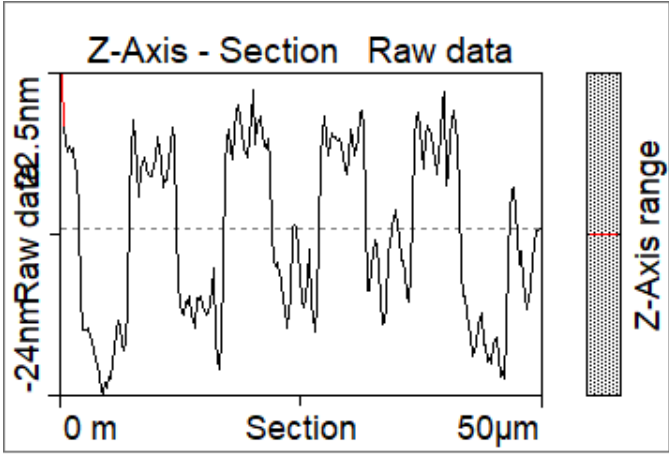


Fig. 7. Cross section of the grid sample - Periodicity

The %error between the actual manufacturer periodicity and the measured periodicity is:

periodicity along the Y axis:

$$\%error = \frac{|9.863\mu m - 10.000\mu m|}{10.000\mu m} \times 100\% = 1.37\%$$

Horizontal along the X axis:

$$\%error = \frac{|9.619\mu m - 10.000\mu m|}{10.000\mu m} \times 100\% = 3.81\%$$

Using the zooming tool, we selected this area Figure 8.

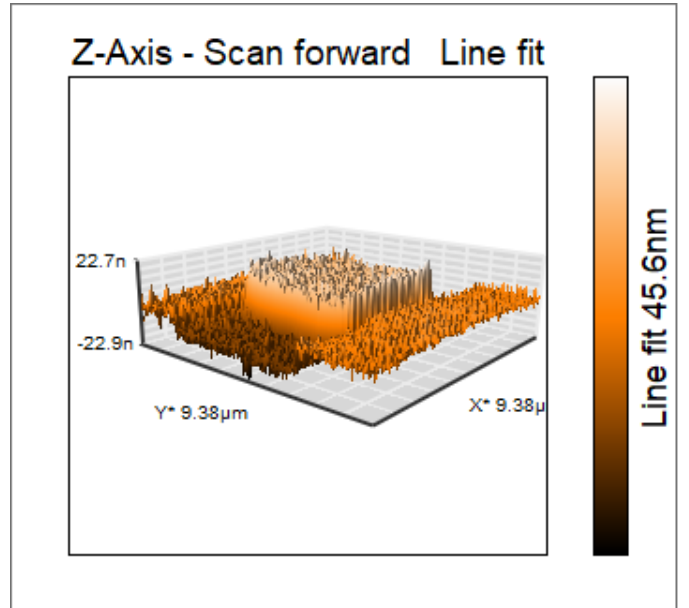


Fig. 9. 3D image of the zoomed grid sample

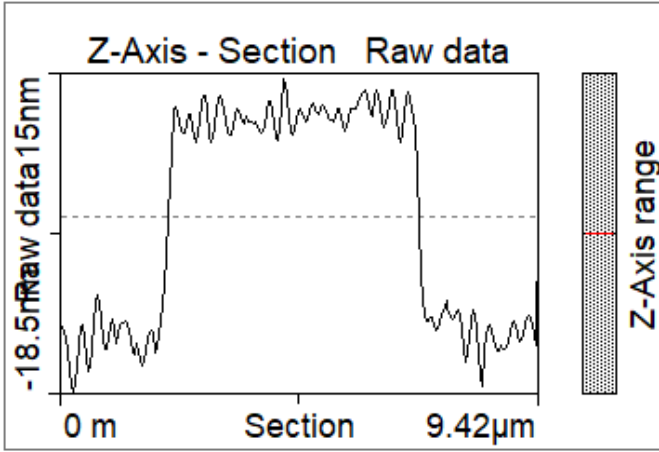


Fig. 10. The cross-section of the zoomed grid sample

We obtained some relevant dimensions of this zoomed sample:

TABLE VI. ZOOMED SAMPLE SCANNING PARAMETERS

	Length(μm)	delta z(nm)	Width	Height
Y	5.024	8.52	659.2 nm	4.98 μm
X	5.073	9.598	5.054 μm	439.5 nm

The %error between the actual manufacturer square's length and the measured square's length is:

Square's length along the Y axis:

$$\%error = \frac{|5.024\mu m - 5.000\mu m|}{5.000\mu m} \times 100\% = 0.48\%$$

Square's length along the X axis:

$$\%error = \frac{|5.073\mu m - 5.000\mu m|}{5.000\mu m} \times 100\% = 1.46\%$$

2) CD sample: :

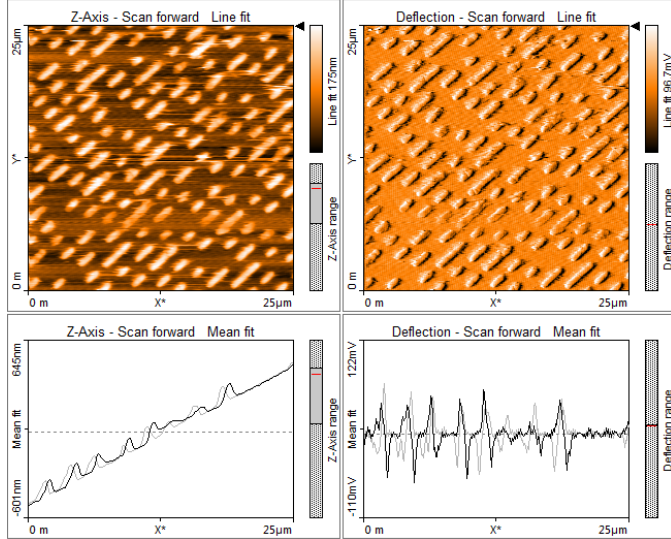


Fig. 11. CD sample

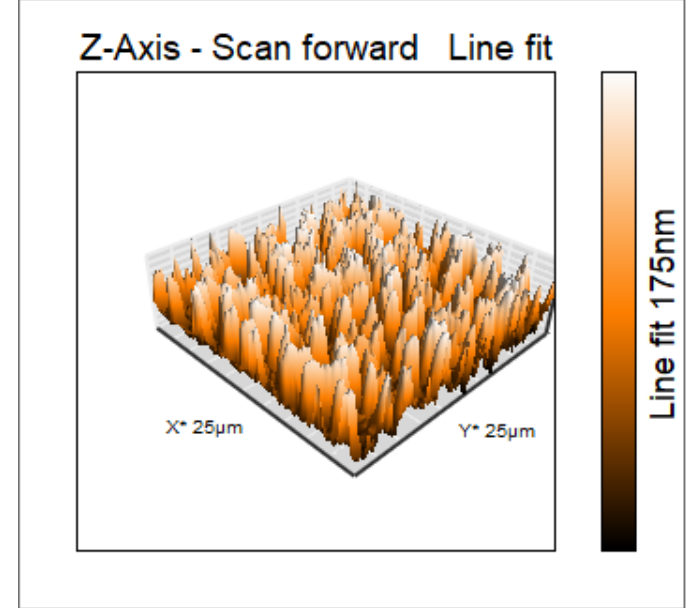


Fig. 12. 3D view of the CD sample

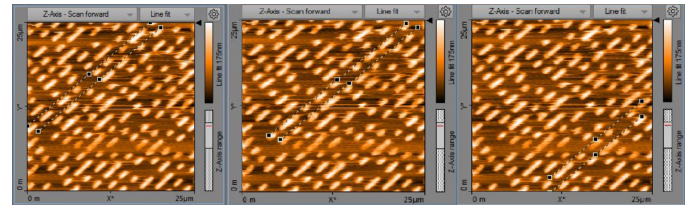


Fig. 13. Measuring Periodicity of the CD sample

TABLE VII. PERIODICITY SCANNING PARAMETER FOR THE CD SAMPLE

	Periodicity (μm)
1st	1.603
2nd	1.500
3rd	1.662
Average	1.588
Standard Deviation	0.0819

We found that the nominal distance between tracks on CD media is  $1.6 \mu m$  [3]

So the %error between the nominal distance and the measured periodicity distance is:

$$\%error = \frac{|1.588\mu m - 1.600\mu m|}{1.600\mu m} \times 100\% = 0.75\%$$

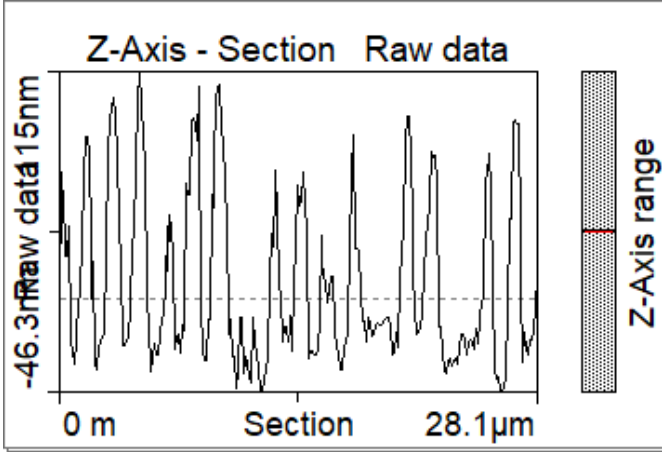


Fig. 14. Cross section of the CD sample

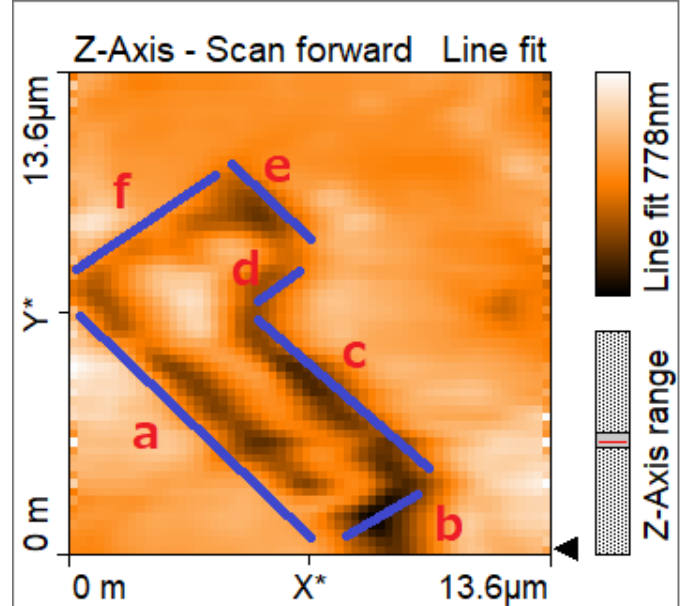


Fig. 17. Dimensions of the SCA Sample

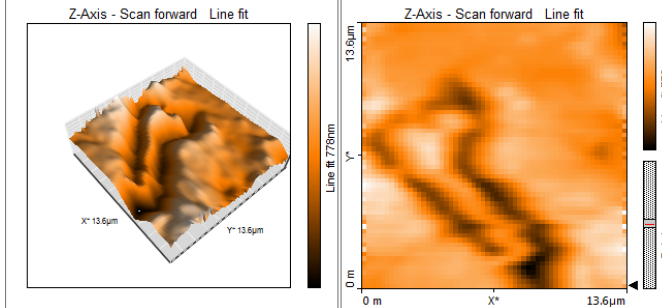


Fig. 15. SCA Sample

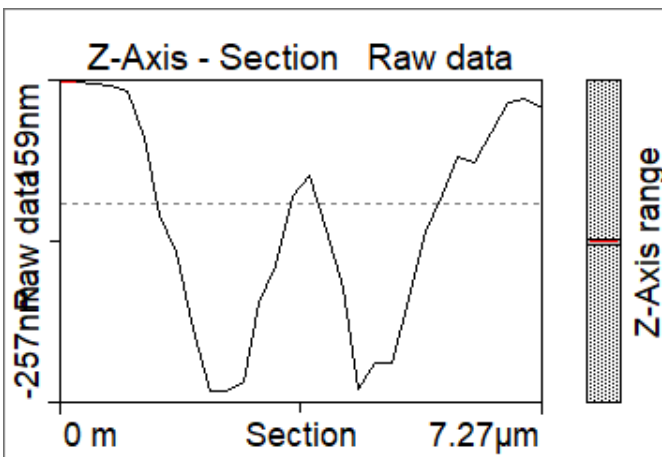


Fig. 16. Cross section of the SCA Sample

TABLE VIII. SCA DIMENSIONS MEASUREMENTS

side	a	b	c	d	e	f
Length $\mu\text{m}$	10.46	2.496	6.915	2.523	3.042	5.451

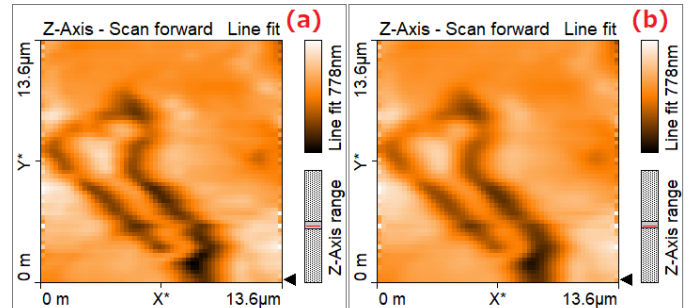


Fig. 18. (a) unfiltered scan vs (b) glitch and noise filter applied on SCA scan image

We calculated the area roughness using the software, such that the data are calculated according to the following formulas:

The Roughness Average,  $S_a$

$$S_a = \frac{1}{N} \sum_{l=1}^{N-1} |z(x_l)|$$

The Mean Value,  $S_m$

$$S_a = \frac{1}{N} \sum_{l=1}^{N-1} z(x_l)$$

The Root Mean Square,  $S_q$

$$S_q = \sqrt{\frac{1}{N} \sum_{l=1}^{N-1} (z(x_l))^2}$$

The Valley depth,  $S_v$

$$S_v = \text{lowest value}$$

The Peak Height,  $S_p$

$$S_p = \text{highest value}$$

The Peak-Valley Height,  $S_y$

$$S_y = S_p - S_v$$

TABLE IX. AREA ROUGHNESS MEASUREMENTS FOR SCA SAMPLE

Parameter	Unfiltered image	Filtered Image
Area( $\mu\text{m}^2$ )	186.2	186.2
$S_a(\text{nm})$	88.652	83.107
$S_q(\text{nm})$	119.43	111.17
$S_y(\text{nm})$	1040.6	1100.1
$S_p(\text{nm})$	573.56	711.74
$S_v(\text{nm})$	-467.01	-388.34
$S_m(\text{fm})$	-20.569	-20.488

### B. Discussion of results

For the three scanned samples, we obtained several parameters for each sample. For the Grid sample, we calculated the average periodicity after taking several measurements by summing all the measured lengths by the total number of readings. We found that periodicity along the Y axis has %error of 1.37% compared to the manufacturer periodicity; however, we found that the error in the periodicity along the Y axis is less than the %error along the X axis of 3.81%. We think that this kind of error is due to an error in the probe in the X scanning direction.

For the CD sample, we calculated the error difference to be %error of 0.75% between the known nominal distance between tracks on CD media is 1.6  $\mu\text{m}$ , and from our scanned sample which has the average distance of 1.588  $\mu\text{m}$ .

Lastly, for SCA sample, because our SCA sample is uneven and it has peaks and valleys, having only the average roughness is not enough because it's just the mean of the absolute sum of heights, so having more parameters information help us to fully distinguish the surface. [4] In the root mean square roughness, we can see that it's similar to the average but in this case we are squaring the heights values makes it's more sensitive to the topology of the surface. For more sophisticated parameters, (peak height, valley depth, the peak valley height), are being used to characterize the surface like finding a deep crack or a sharp peak that could affect the usage of the sample. Referring to table IX, we found that the roughness values for the filtered image are showing the higher precision in comparison to unfiltered image.

### V. CONCLUSION

In conclusion, the experiment achieved its goals in which we learnt how to adjust, calibrate, and operate an AFM and we used it to take multiple scans of the provided samples (Grid, CD and SCA samples), we also learnt how to analyze the obtained data from the scanned images which are produced using the software Nanosurf.

For the Grid sample, the manufacture's parameters are 5  $\mu\text{m}$  square pattern with a 10  $\mu\text{m}$  periodicity. We found that periodicity along the Y axis has %error of 1.37% which is less than the %error along the X axis of 3.81%. Also, from the zooming area of the grid, we found that the square's length along the Y axis has %error of 0.48% which is less than the %error along the X axis of 1.46%. For the CD sample, we know that the nominal distance between tracks on CD media is 1.6  $\mu\text{m}$ , and from our scanned sample, the average distance between tracks is 1.588  $\mu\text{m}$ , which has %error of 0.75%. Lastly, for SCA chip sample, zooming into the L shaped part was challenging as it took time for to get the correct area scanned. However, we ended up using the larger area and we used "cut area" feature to study the L-shaped element.

### REFERENCES

- [1] Meinander, K., Growth and Modification of Cluster-Assembled Thin Films. 2018.
- [2] Binnig, G.; Quate, C. F.; Gerber, C. Phys. Rev. Lett. 1986, 56, 930-933.
- [3] Sokolyanskaya, I. (2001). Separation Between Tracks on a CD - The Physics Factbook. Retrieved from <https://hypertextbook.com/facts/2001/InnaSokolyanskaya2.shtml>
- [4] Measurement of the Nanoscale Roughness by Atomic Force Microscopy: Basic Principles and Applications R.R.L. De Oliveira, D.A.C. Albuquerque, T.G.S. Cruz, F.M. Yamaji and F.L. Leite. Federal University of São Carlos, Campus Sorocaba, Brazil.